0023-6837/02/8204-425$03.00/0
LABORATORY INVESTIGATION
Vol. 82, No. 4, p. 425, 2002
Printed in U.S.A.

Cell-Specific Nitric Oxide Synthase-Isoenzyme Expression and Regulation in Response to Endotoxin in Intact Rat Lungs

Monika Ermert, Clemens Ruppert, Andreas Günther, Hans-Rainer Duncker, Werner Seeger, and Leander Ermert

Department of Pathology (ME, LE), the Institute of Anatomy and Cell Biology (H-RD), and the Department of Internal Medicine (CR, AG, WS), Justus-Liebig-University Giessen, Giessen, Germany

SUMMARY: Nitric oxide (NO) produced by NO synthase (NOS) serves as a ubiquitous mediator molecule involved in many physiologic lung functions, including regulation of vascular and bronchial tone, immunocompetence, and neuronal signaling. On the other hand, excessive and inappropriate NO synthesis in inflammation and sepsis has been implicated in vascular abnormalities and cell injury. At least three different NOS isoforms (neuronal/brain [bNOS], inducible [iNOS], and endothelial [eNOS]) have been described, which are all expressed in normal lung tissue. We investigated the cell-specific expression of bNOS, iNOS, and eNOS in perfused control rat lungs and lungs undergoing stimulation with endotoxin in the presence and absence of plasma constituents. Lung immunohistochemistry and quantitative evaluation of staining intensity showed endotoxin-induced increase in iNOS expression in particular in bronchial epithelial cells, cells of the bronchus-associated lymphoid tissue (BALT), alveolar macrophages, and vascular smooth muscle cells in a time- and dose-dependent fashion. In endothelial cells, which did not express iNOS at baseline, newly induced iNOS was found in response to endotoxin. In contrast, expression of eNOS was markedly suppressed under endotoxin challenge, particularly in bronchial epithelium, BALT, and alveolar macrophages but also in vascular smooth muscle cells and endothelial cells. eNOS expression in bronchial smooth muscle cells was not altered. In contrast to iNOS and eNOS, cellular expression of bNOS in epithelial cells, nerve fibers, BALT, and endothelial cells did not change in response to endotoxin. All changes in NOS regulation were found to be independent of plasma constituents. We conclude that endotoxin exerts a profound impact on the cell-specific NOS regulation in a large number of lung cell types. Prominent features include de novo synthesis or up-regulation of iNOS, in contrast to down-regulation of eNOS, which may well contribute to vascular abnormalities, inflammatory sequelae, and loss of physiologic functions in septic lung failure. (*Lab Invest 2002, 82:425–441*).

Nitric oxide (NO) generated by NO synthase (NOS) plays an important role in physiologic and pathophysiologic processes in the lung including vasotone and bronchotone regulation, neurotransmission, immune defense, and mucin secretion (Gaston et al, 1994; Moncada et al, 1991). Three isoenzymes of NOS have been described (Gaston et al, 1994; Moncada and Higgs, 1993): the neuronal isoform bNOS (NOS-1) and an endothelial isoform eNOS (NOS-3) as constitutive isoenzymes, and a mitogen-inducible isoform iNOS (NOS-2). Cellular expression of bNOS and eNOS in different cell types of normal lung tissue and pulmonary cell cultures has been reported earlier (Kobzik et al, 1993; Shaul et al, 1994; Sherman et al, 1999). Cellular expression of iNOS in the lung parenchyma has so far only been observed after experimental endotoxin stimulation or in sections from patients suffering from inflammatory lung disease (Kobzik et al, 1993; Robbins et al, 1994; Tracey et al, 1994). However, recently all three NOS isoforms were shown by immunohistochemistry to be expressed in the developing lung, and all were assumed to contribute to NO generation functioning in normal lung physiology (Sherman et al, 1999; Xue et al, 1996). A recent study performed in human airway tissue originating from patients with bronchial carcinoma undergoing lung resection showed iNOS expression in bronchial epithelial cells (Watkins et al, 1997).

Extensive production of NO has been assumed to be a key event in the pathogenesis of several inflammatory lung diseases, such as sepsis-induced lung injury and asthma (Hamid et al, 1993; Hinder et al, 1999; Kristof et al, 1998). The inducible isoform iNOS can be activated by bacterial lipopolysaccharides (LPS, endotoxin) and cytokines (Kristof et al, 1998; Nakayama et al, 1992; Robbins et al, 1994) and—via excess NO formation—may cause inappropriate vasodilation, which is a key feature in septic organ failure (Stewart et al, 1995; Ullrich et al, 1999). In addition, iNOS-dependent excessive NO generation may induce tissue damage through the formation of peroxynitrite, and such an event has been implicated in the pathogenesis of LPS-induced lung injury (Kooy et

Received October 30, 2001.
This work was supported by the Deutsche Forschungsgemeinschaft (SFB 547 "Kardiopulmonales Gefäßsystem").
Address reprint requests to: Dr. Leander Ermert, Institut fuer Anatomie und Zellbiologie, Aulweg 123, 35385 Giessen, Germany. E-mail: leander.ermert@anatomie.med.uni-giessen.de

al, 1995; van der Vliet et al, 1999; Wizemann et al, 1994). Studies in mice deficient in iNOS gene activity were shown to be more resistant to LPS-induced acute lung injury than wild-type animals (Kristof et al, 1998; Weimann et al, 1999).

Because of the vasodilatory effects of NO, inhalation of this agent has been used as a therapeutic approach to decrease the pulmonary vascular resistance in well-ventilated, ie, NO-accessible lung areas, and thereby improve oxygenation in patients with acute respiratory distress syndrome (ARDS) (Michael et al, 1998; Payen, 1998; Troncy et al, 1998). Unfortunately, NO inhalation, although initially improving gas exchange, did not lead to sustained improvement of oxygenation compared with conventional therapy in the hitherto performed controlled studies (Michael et al, 1998; Payen, 1998). Nonvasodilation-related effects of inhaled NO, currently not well understood, have been suggested to explain this finding. Moreover, too little information exists about the regulation of the different NOS isoenzymes, and thus the background of endogenous NO formation in ARDS and septic lung failure is still unclear (Payen, 1998). Such regulation may apparently include iNOS and enhanced expression of iNOS in several cell types such as epithelial cells (Kobzik et al, 1993; Warner et al, 1995; Watkins et al, 1997), alveolar macrophages (Kobzik et al, 1993; Tracey et al, 1994), or endothelial cells (Kobzik et al, 1993; MacNaul and Hutchinson, 1993), which has been reported in several studies in response to mitogen stimulation. In addition, regulation of eNOS and bNOS may be affected, however, only minimal information about the regulation of these constitutive isoforms in response to LPS or cytokines currently exists. Some recent evidence suggests that the activity of the constitutive eNOS may be down-regulated during inflammation (MacNaul and Hutchinson, 1993; Schwartz et al, 1997).

In the present study, we assessed cell type–specific regulation of the different NOS isoenzymes in rat lung tissue in response to intravascularly applied LPS by a previously described method of in situ microdensitometry (Ermert et al, 2000a, 2001). In a recent study using this technique, cyclooxygenase-2 (Cox-2) was shown to be time-dependently and LPS dose-dependently up-regulated in different cells of isolated rat lungs challenged with endotoxin (Ermert et al, 2000b). Interestingly, several cell types such as vascular smooth muscle cells (VSMC) of large arteries, endothelial cells, or bronchial smooth muscle cells displayed such Cox-2 up-regulation only in the presence of plasma constituents in the buffer perfusate. This plasma dependence was correlated with the lack of expression of membrane CD14 in these cell types, again demonstrated by immunohistochemistry (Ermert et al, 2000b). Several effects of LPS are known to be mediated by the plasma protein LBP (LPS-binding protein) and the membrane receptor CD14 (Pugin et al, 1993; Tobias et al, 1989; Ulevitch, 1993). Moreover, a soluble form of CD14 has been described that forms complexes with LPS and LBP and may then bind to cells negative for membrane CD14 (Frey et al, 1992; Pugin et al, 1993). Recently, additional LPS receptors (CD55, Toll-like receptors) have been detected, which may serve as coreceptor(s) for CD14 providing an intracellular domain for signal transduction, because CD14 is void of such a domain (El Samalouti et al, 1999; Qureshi et al, 1999; Yang et al, 1998).

Against this background, the current investigation again used perfused rat lungs, stimulated with LPS in the absence or presence of plasma constituents, to address the profile of lung cellular NOS expression under baseline conditions and in response to microbial challenge.

Results

Immunohistochemistry of NOS isoenzymes shows constitutive expression of all three NOS isoenzymes in rat lung tissue (Fig. 1). Staining was absent in sections where the primary antibody was omitted or nonspecific immune serum was used (Fig. 1D). Background staining was low (mean gray value <100). Nerve fibers, which were positive for all three isoenzymes (Tables 1 to 3), were not measured by image analysis because they were not regularly present in all lung sections.

eNOS

Control Lungs. In normal rat lung tissue, bronchial epithelial cells exhibited a strong eNOS immunostaining, which could be detected in all large and small bronchi (Table 1, a and b; Fig. 2A). Similarly, endothelial cells were strongly stained (Fig. 2, C and E). In addition bronchial smooth muscle cells (Fig. 2A) and VSMCs of fully muscular and partially muscular vessels (Figs. 1C and 2E) showed marked immunoreactivity. Smooth muscle cells of large arteries at the hilum and myocytes of large hilar veins were not stained (Table 1, a and b; Fig. 2C). In addition, peribronchial and perivascular nerve fibers, cells within the bronchus-associated lymphoid tissue (BALT), and alveolar macrophages exhibited positive staining for eNOS (Table 1, a and b). No difference between controls with buffer-perfusion and those with buffer/plasma-perfusion was noted.

Expression of eNOS after LPS. In response to LPS, a significant decrease in eNOS staining intensity was detected within 1 hour in nearly all cell types that expressed eNOS under baseline conditions. Decrease in staining intensity is visualized by pseudocolor depiction, eg, in bronchial epithelial cells of large bronchi (Fig. 2, A and B), endothelial cells (Fig. 2, C and D), or VSMCs of small muscular vessels (Fig. 2, E and F). The decrease in staining intensity occurred within 1 hour and was further enhanced within 2 hours of LPS incubation (Table 1, a and b; Fig. 4). In addition, the LPS-induced decrease in eNOS staining intensity was dose-dependent and already evident upon low-dose LPS challenge (50 ng/ml LPS), in particular in bronchial epithelial cells, alveolar macrophages, and VSMCs (Table 1, a and b).

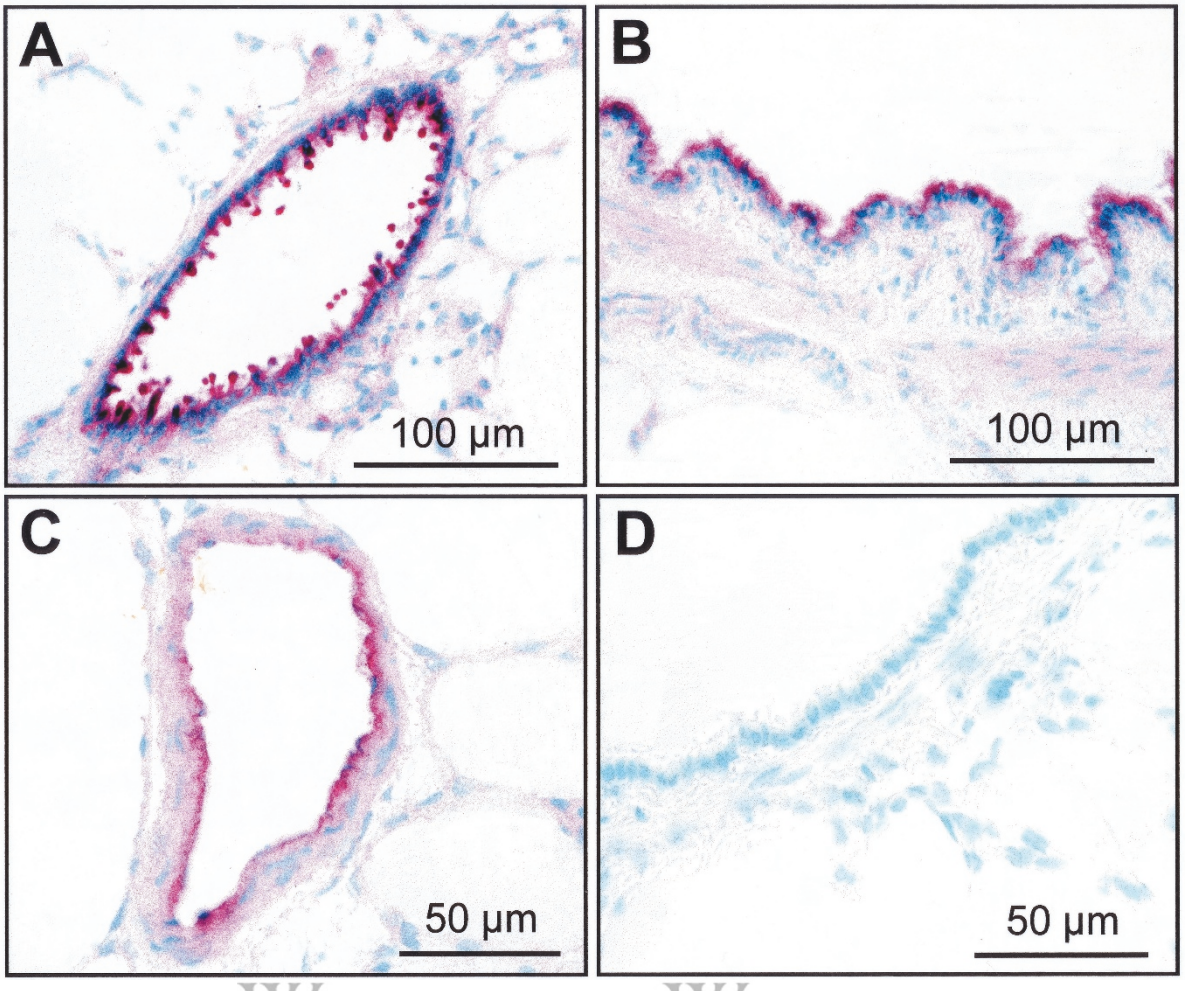

Figure 1.

Immunohistochemical localization of neuronal/brain nitric oxide synthase (bNOS) (A), inducible (i)NOS (B) and endothelial (e)NOS (C) in normal rat lung tissue. (A). Strong bNOS immunostaining was detected in bronchial epithelial cells of small bronchioli within the alveolar tissue. (B) Constitutive iNOS expression was found in bronchial epithelium and bronchial smooth muscle cells. Vascular smooth muscle cells (VSMCs) and especially endothelial cells of pulmonary vessels showed positive immunostaining for eNOS (C). Control staining with nonspecific immune serum shows no staining reaction (D).

Staining intensity was not found to be decreased after LPS application in bronchial smooth muscle cells (Table 1, a and b; Fig. 2, A and B). Immunostaining of eNOS was newly detected in mast cells located in the perivascular and peribronchial connective tissue (Table 1, a and b; Fig. 4). Moreover, in mast cells a significant increase of eNOS expression was noted in groups exposed to 10,000 ng/ml LPS for 2 hours as compared with 1 hour. There was no difference in the cellular eNOS expression and regulation pattern in groups perfused in the absence (Table 1a) versus the presence (Table 1b) of 1.5% plasma.

iNOS

Control Lungs. Strong iNOS immunoreactivity was localized to bronchial epithelial cells mainly of large first- and second-generation bronchi within normal rat lung tissue (Table 2, a and b; Figs. 1B and 3A). In addition, cells of the BALT, single cells within the alveolar septum, and alveolar macrophages (Fig. 3C) showed positive immunoreactivity. Bronchial smooth muscle cells (Figs. 1B and 3A), smooth muscle cells of fully muscular and partially muscular vessels, and myocytes of large hilar veins (Fig. 3E) displayed moderate iNOS immunostaining (Table 2, a and b) in contrast to large arteries, which were not stained. Perivascular leukocytes, mast cells in the perivascular and peribronchial connective tissue, and endothelial cells were not stained in control lungs. In accordance with eNOS and bNOS immunostaining, no difference between controls with buffer-perfusion and those with buffer/plasma-perfusion was noted.

Expression of iNOS after LPS. After LPS stimulation, iNOS expression was increased in all cell types that showed iNOS immunoreactivity in control lungs (Table 2, a and b). The increase in staining intensity of iNOS displayed time and dose dependency (Fig. 5). Even challenge with low-dose LPS (50 ng/ml) sufficed to provoke some increase in staining intensity, which was, however, not statistically significant in most cell types.

Table 1a. Quantification of eNOS Staining Intensity—Experiments in the Absence of Plasma (Mean Gray Values)

Structures	Control	50 ng/ml LPS (2 hr)	1,000 ng/ml LPS		10,000 ng/ml LPS	
			1 hr	2 hr	1 hr	2 hr
Bronchial epithelial cells of bronchi (1st and 2nd generation)	2106 ± 378	1255 ± 196***	1490 ± 314***	1287 ± 196***	1400 ± 598***	921 ± 153***
Bronchial epithelial cells of bronchi (3rd generation) and bronchioli	1888 ± 464	1027 ± 187***	1174 ± 237***	1119 ± 120***	1480 ± 214**	1080 ± 126***
Bronchial smooth muscle cells	1502 ± 324	1371 ± 348	1786 ± 291	1583 ± 409	1684 ± 362	1388 ± 415
Nerve fibers	s.p.	s.p.	s.p.	s.p.	s.p.	s.p.
Cells of the BALT	1446 ± 261	1457 ± 56	1587 ± 412	1002 ± 233	1363 ± 93	592 ± 161***
Single cells in the alveolar septum	n.d.	n.d.	n.d.	n.d.	n.d.	n.d.
Alveolar macrophages	1508 ± 320	642 ± 180***	1031 ± 213***	655 ± 149***	894 ± 254***	786 ± 244***
Perivascular leukocytes	n.d.	n.d.	n.d.	n.d.	n.d.	n.d.
Mast cells	n.d.	1514 ± 466	1388 ± 247	1629 ± 346	851 ± 223	1744 ± 305###
Endothelial cells	2362 ± 502	2203 ± 401	1800 ± 409***	1214 ± 328***	1117 ± 301***	1074 ± 291***
Vascular smooth muscle cells of large arteries at the hilum	n.d.	n.d.	n.d.	n.d.	n.d.	n.d.
Vascular smooth muscle cells of fully muscular vessels	1934 ± 376	1219 ± 295***	1172 ± 393***	1179 ± 182***	1510 ± 200*	1119 ± 174***
Vascular smooth muscle cells of partially muscular vessels	1598 ± 389	1155 ± 469**	1337 ± 174	960 ± 240***	1209 ± 172	881 ± 179***
Myocytes of large veins at the hilum	n.d.	n.d.	n.d.	n.d.	n.d.	n.d.

n.d., staining not detected; s.p., staining positive (occurrence too low for measurement).

Mean ± SEM values for each group of buffer-perfused lungs is given. Each group comprised five independent lung experiments, and cross sections from three randomly selected tissue blocks originating from different lung lobes were investigated per lung.

* $p < 0.05$, ** $p < 0.01$, *** $p < 0.001$ versus control; # $p < 0.05$, ## $p < 0.01$, ### $p < 0.001$ versus respective 1-hr value.

Table 1b. Quantification of eNOS Staining Intensity—Experiments in the Presence of Plasma (Mean Gray Values)

Structures	Control	50 ng/ml LPS (2 hr)	1,000 ng/ml LPS		10,000 ng/ml LPS	
			1 hr	2 hr	1 hr	2 hr
Bronchial epithelial cells of bronchi (1st and 2nd generation)	2543 ± 450	1234 ± 153***	1127 ± 227***	1216 ± 113***	1368 ± 288***	1166 ± 311***
Bronchial epithelial cells of bronchi (3rd generation) and bronchioli	1933 ± 463	1095 ± 106***	1313 ± 282**	962 ± 110***	1234 ± 501***	1200 ± 163***
Bronchial smooth muscle cells	1882 ± 327	1592 ± 426	1723 ± 296	1609 ± 337	1740 ± 442	1465 ± 248
Nerve fibers	s.p.	s.p.	s.p.	s.p.	s.p.	s.p.
Cells of the BALT	1502 ± 303	1278 ± 253	1462 ± 131	962 ± 203**	913 ± 355**	922 ± 183**
Single cells in the alveolar septum	n.d.	n.d.	n.d.	n.d.	n.d.	n.d.
Alveolar macrophages	1402 ± 336	738 ± 239***	802 ± 150**	696 ± 174**	1086 ± 216	884 ± 221**
Perivascular leukocytes	n.d.	n.d.	n.d.	n.d.	n.d.	n.d.
Mast cells	n.d.	1536 ± 381	1159 ± 412	1204 ± 286	1030 ± 357	1745 ± 216##
Endothelial cells	2441 ± 368	2147 ± 271	1656 ± 107**	1050 ± 330***	1087 ± 364***	991 ± 256***
Vascular smooth muscle cells of large arteries at the hilum	n.d.	n.d.	n.d.	n.d.	n.d.	n.d.
Vascular smooth muscle cells of fully muscular vessels	2073 ± 181	1038 ± 38***	1393 ± 216***	926 ± 220***	1559 ± 294**	1074 ± 226***
Vascular smooth muscle cells of partially muscular vessels	1663 ± 193	1154 ± 187**	1193 ± 272**	939 ± 118***	1386 ± 339	984 ± 294***
Myocytes of large veins at the hilum	n.d.	n.d.	n.d.	n.d.	n.d.	n.d.

n.d., staining not detected; s.p., staining positive (occurrence too low for measurement).

Mean ± SEM values for each group of buffer-perfused lungs is given. Each group comprised five independent lung experiments, and cross sections from three randomly selected tissue blocks originating from different lung lobes were investigated per lung.

* $p < 0.05$, ** $p < 0.01$, *** $p < 0.001$ versus control; # $p < 0.05$, ## $p < 0.01$, ### $p < 0.001$ versus respective 1-hr value.

Table 2a. Quantification of iNOS Staining Intensity—Experiments in the Absence of Plasma (Mean Gray Values)

Structures	Control	50 ng/ml LPS (2 hr)	1,000 ng/ml LPS		10,000 ng/ml LPS	
			1 hr	2 hr	1 hr	2 hr
Bronchial epithelial cells of bronchi (1st and 2nd generation)	1789 ± 293	2062 ± 375*	2062 ± 251**	2304 ± 267***	2538 ± 289***	2413 ± 233***
Bronchial epithelial cells of bronchi (3rd generation) and bronchioli	1364 ± 311	1662 ± 434	1690 ± 343	2097 ± 657***	1985 ± 241***	1806 ± 298
Bronchial smooth muscle cells	1306 ± 140	1518 ± 218	1801 ± 389***	1932 ± 183***	1846 ± 230***	2147 ± 378***
Nerve fibers	s.p.	s.p.	s.p.	s.p.	s.p.	s.p.
Cells of the BALT	1430 ± 304	1479 ± 205	2021 ± 236***	1736 ± 253*	2180 ± 282***	1737 ± 429**
Single cells in the alveolar septum	1294 ± 394	1456 ± 239	1461 ± 240	1574 ± 284	1809 ± 312***	1701 ± 309**
Alveolar macrophages	1034 ± 214	1403 ± 236	1837 ± 260***	2052 ± 563***	1699 ± 299***	1822 ± 332***
Perivascular leukocytes	n.d.	n.d.	1184 ± 191	1550 ± 151###	1414 ± 302	1967 ± 479###
Mast cells	n.d.	n.d.	n.d.	n.d.	n.d.	n.d.
Endothelial cells	n.d.	1457 ± 284	1805 ± 407	2164 ± 350###	2372 ± 341	2294 ± 184
Vascular smooth muscle cells of large arteries at the hilum	n.d.	n.d.	n.d.	n.d.	n.d.	n.d.
Vascular smooth muscle cells of fully muscular vessels	1110 ± 172	1326 ± 309	1441 ± 331***	1637 ± 204***	1626 ± 208***	1718 ± 345***
Vascular smooth muscle cells of partially muscular vessels	1268 ± 203	1251 ± 311	1349 ± 361	1732 ± 237***	1519 ± 157	1792 ± 165***
Myocytes of large veins at the hilum	423 ± 316	1430 ± 251	2476 ± 456***	2478 ± 257***	1947 ± 272***	1968 ± 259***

n.d., staining not detected; s.p., staining positive (occurrence too low for measurement).

Mean ± SEM values for each group of buffer-perfused lungs is given. Each group comprised five independent lung experiments, and cross sections from three randomly selected tissue blocks originating from different lung lobes were investigated per lung.

* $p < 0.05$, ** $p < 0.01$, *** $p < 0.001$ versus control; # $p < 0.05$, ## $p < 0.01$, ### $p < 0.001$ versus respective 1-hr value.

Table 2b. Quantification of iNOS Staining Intensity—Experiments in the Presence of Plasma (Mean Gray Values)

Structures	Control	50 ng/ml LPS (2 hr)	1,000 ng/ml LPS		10,000 ng/ml LPS	
			1 hr	2 hr	1 hr	2 hr
Bronchial epithelial cells of bronchi (1st and 2nd generation)	1816 ± 375	1905 ± 293	2045 ± 214*	2673 ± 412***	2541 ± 356***	2548 ± 348***
Bronchial epithelial cells of bronchi (3rd generation) and bronchioli	1270 ± 367	1493 ± 368	1493 ± 298	1729 ± 430*	1464 ± 361	1443 ± 303*
Bronchial smooth muscle cells	1440 ± 299	1689 ± 214	1500 ± 171	1976 ± 357***	1932 ± 301***	2140 ± 293***
Nerve fibers	s.p.	s.p.	s.p.	s.p.	s.p.	s.p.
Cells of the BALT	1391 ± 187	1628 ± 363	1757 ± 318**	2233 ± 248***	2226 ± 185***	1449 ± 110
Single cells in the alveolar septum	1333 ± 376	1440 ± 188	1442 ± 275	1985 ± 27***	1701 ± 309**	1575 ± 283
Alveolar macrophages	1072 ± 261	1190 ± 313	1554 ± 330	2021 ± 393***	1806 ± 507***	2078 ± 333***
Perivascular leukocytes	n.d.	n.d.	1167 ± 85	1856 ± 247###	1687 ± 550	1464 ± 324
Mast cells	n.d.	n.d.	n.d.	n.d.	n.d.	n.d.
Endothelial cells	n.d.	1345 ± 239	1740 ± 397	2491 ± 275###	2045 ± 305	1936 ± 360
Vascular smooth muscle cells of large arteries at the hilum	n.d.	n.d.	n.d.	n.d.	n.d.	n.d.
Vascular smooth muscle cells of fully muscular vessels	1245 ± 282	1302 ± 305	1393 ± 150	1989 ± 226***	1712 ± 237**	1809 ± 360***
Vascular smooth muscle cells of partially muscular vessels	1373 ± 296	1327 ± 256	1420 ± 289	1942 ± 378***	1571 ± 450	1794 ± 168***
Myocytes of large veins at the hilum	1376 ± 352	1276 ± 363	1794 ± 242***	2619 ± 304***	2068 ± 395***	2348 ± 292***

n.d., staining not detected; s.p., staining positive (occurrence too low for measurement).

Mean ± SEM values for each group of buffer-perfused lungs is given. Each group comprised five independent lung experiments, and cross sections from three randomly selected tissue blocks originating from different lung lobes were investigated per lung.

* $p < 0.05$, ** $p < 0.01$, *** $p < 0.001$ versus control; # $p < 0.05$, ## $p < 0.01$, ### $p < 0.001$ versus respective 1-hr value.

Table 3a. Quantification of bNOS Staining Intensity—Experiments in the Absence of Plasma (Mean Gray Values)

Structures	Control	1,000 ng/ml LPS (2 hr)	10,000 ng/ml LPS 1 hr	10,000 ng/ml LPS 2 hr
Bronchial epithelial cells of bronchi (1st and 2nd generation)	2009 ± 395	1965 ± 325	1763 ± 342	1970 ± 194
Bronchial epithelial cells of bronchi (3rd generation) and bronchioli	2698 ± 386	2513 ± 330	2610 ± 287	2629 ± 249
Bronchial smooth muscle cells	n.d.	n.d.	n.d.	n.d.
Nerve fibers	s.p.	s.p.	s.p.	s.p.
Cells of the BALT	1350 ± 272	1228 ± 229	1484 ± 341	1256 ± 123
Single cells in the alveolar septum	n.d.	n.d.	n.d.	n.d.
Alveolar macrophages	1718 ± 323	1489 ± 517	1331 ± 336	1715 ± 411
Perivascular leukocytes	n.d.	n.d.	n.d.	n.d.
Mast cells	1727 ± 385	1370 ± 255	1491 ± 403	1784 ± 290
Endothelial cells	1243 ± 335	1346 ± 405	1318 ± 360	1108 ± 210
Vascular smooth muscle cells of large arteries at the hilum	n.d.	n.d.	n.d.	n.d.
Vascular smooth muscle cells of fully muscular vessels	1093 ± 156	904 ± 139	1168 ± 286	1013 ± 197
Vascular smooth muscle cells of partially muscular vessels	n.d.	n.d.	n.d.	n.d.
Myocytes of large veins at the hilum	911 ± 100	953 ± 211	1063 ± 258	1014 ± 154

n.d., staining not detected; s.p., staining positive (occurrence too low for measurement).

Mean ± SEM values for each group of buffer-perfused lungs is given. Each group comprised five independent lung experiments, and cross sections from three randomly selected tissue blocks originating from different lung lobes were investigated per lung.

* $p < 0.05$, ** $p < 0.01$, *** $p < 0.001$ versus control.

Table 3b. Quantification of bNOS Staining Intensity—Experiments in the Presence of Plasma (Mean Gray Value)

Structures	Control	1,000 ng/ml LPS (2 hr)	10,000 ng/ml LPS 1 hr	10,000 ng/ml LPS 2 hr
Bronchial epithelial cells of bronchi (1st and 2nd generation)	1789 ± 553	1899 ± 541	2018 ± 410	1750 ± 277
Bronchial epithelial cells of bronchi (3rd generation) and bronchioli	2523 ± 376	2674 ± 408	2675 ± 236	2504 ± 341
Bronchial smooth muscle cells	n.d.	n.d.	n.d.	n.d.
Nerve fibers	s.p.	s.p.	s.p.	s.p.
Cells of the BALT	1167 ± 155	1281 ± 272	1389 ± 258	1399 ± 393
Single cells in the alveolar septum	n.d.	n.d.	n.d.	n.d.
Alveolar macrophages	1346 ± 246	1207 ± 170	1374 ± 337	1592 ± 417
Perivascular leukocytes	n.d.	n.d.	n.d.	n.d.
Mast cells	1370 ± 255	1898 ± 241	1355 ± 157	1510 ± 575
Endothelial cells	1106 ± 300	1138 ± 420	1200 ± 270	1264 ± 540
Vascular smooth muscle cells of large arteries at the hilum	n.d.	n.d.	n.d.	n.d.
Vascular smooth muscle cells of fully muscular vessels	992 ± 147	1036 ± 407	1128 ± 288	970 ± 345
Vascular smooth muscle cells of partially muscular vessels	n.d.	n.d.	n.d.	n.d.
Myocytes of large veins at the hilum	1010 ± 375	964 ± 231	1033 ± 457	904 ± 144

n.d., staining not detected; s.p., staining positive (occurrence too low for measurement).

Mean ± SEM values for each group of buffer-perfused lungs is given. Each group comprised five independent lung experiments, and cross sections from three randomly selected tissue blocks originating from different lung lobes were investigated per lung.

* $p < 0.05$, ** $p < 0.01$, *** $p < 0.001$ versus control.

Bronchial epithelial cells of large bronchi (Fig. 3, A and B) and myocytes of large hilar veins (Fig. 3, E and F) displayed the highest staining intensities under challenge with LPS as compared with other cell types. In addition, an increase in staining intensity was also evident in bronchial smooth muscle cells (Figs. 3, A and B, and 5) and alveolar macrophages (Figs. 3, C and D, and 5). In VSMC of fully muscular and partially

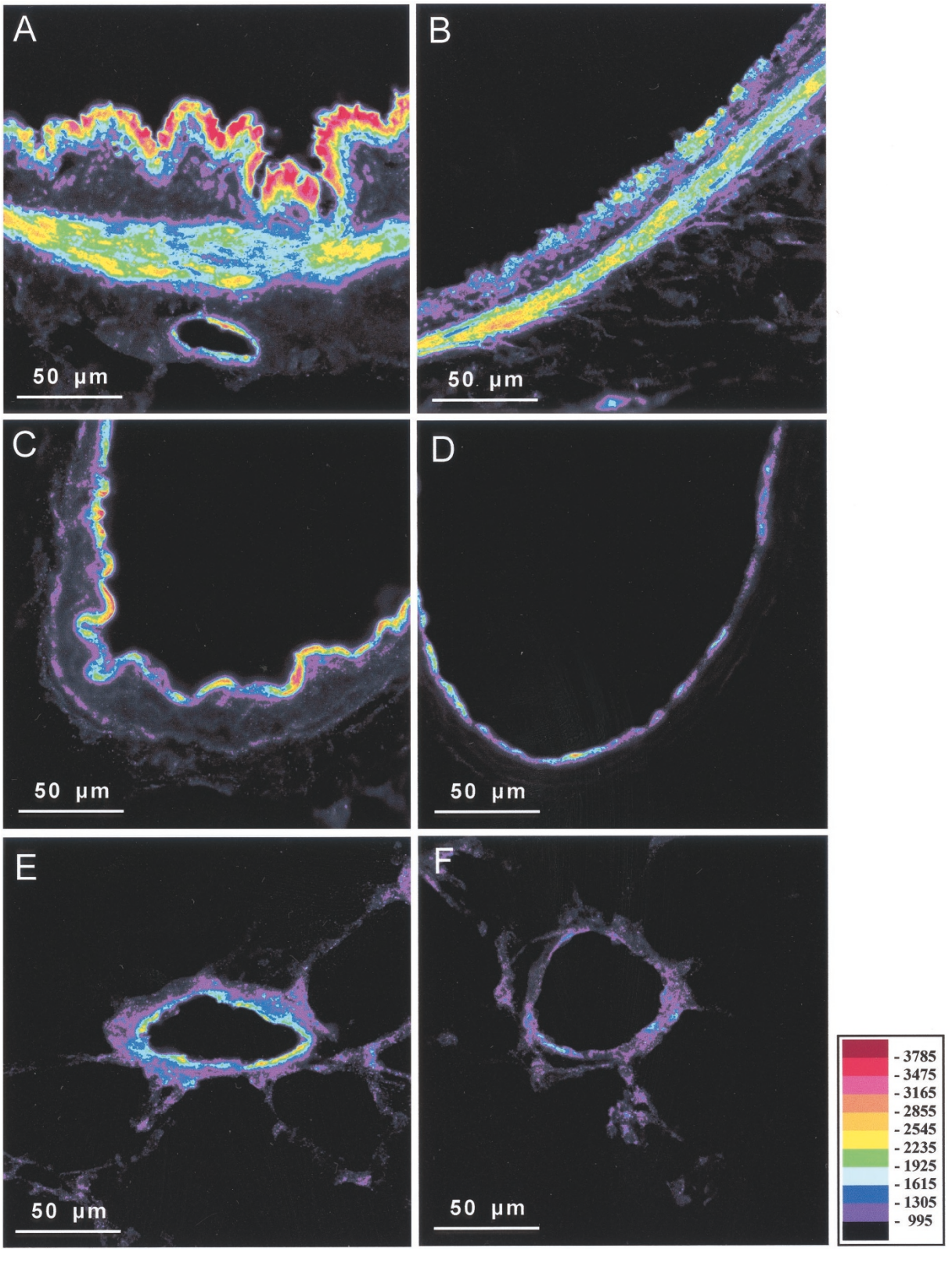

Figure 2.

Image analysis with pseudocolor depiction of immunohistochemical eNOS staining in control (A, C, and E) and lipopolysaccharide (LPS)-stimulated rat lung tissue (B, D, and F). eNOS staining intensity was decreased in bronchial epithelial cells in response to LPS, whereas the expression of this isoenzyme in bronchial smooth muscle cells remained unchanged (B, 1000 ng/ml LPS, 2 hours). Likewise, strong endothelial eNOS expression (C) was found to decrease after LPS challenge (D, 10,000 ng/ml LPS, 2 hours). Note that muscle cells of the artery wall (C and D) are not stained. Staining intensity of VSMC and endothelium of small muscular vessels (E) is markedly decreased in LPS-treated lungs (F, 10,000 ng/ml LPS, 2 hours).

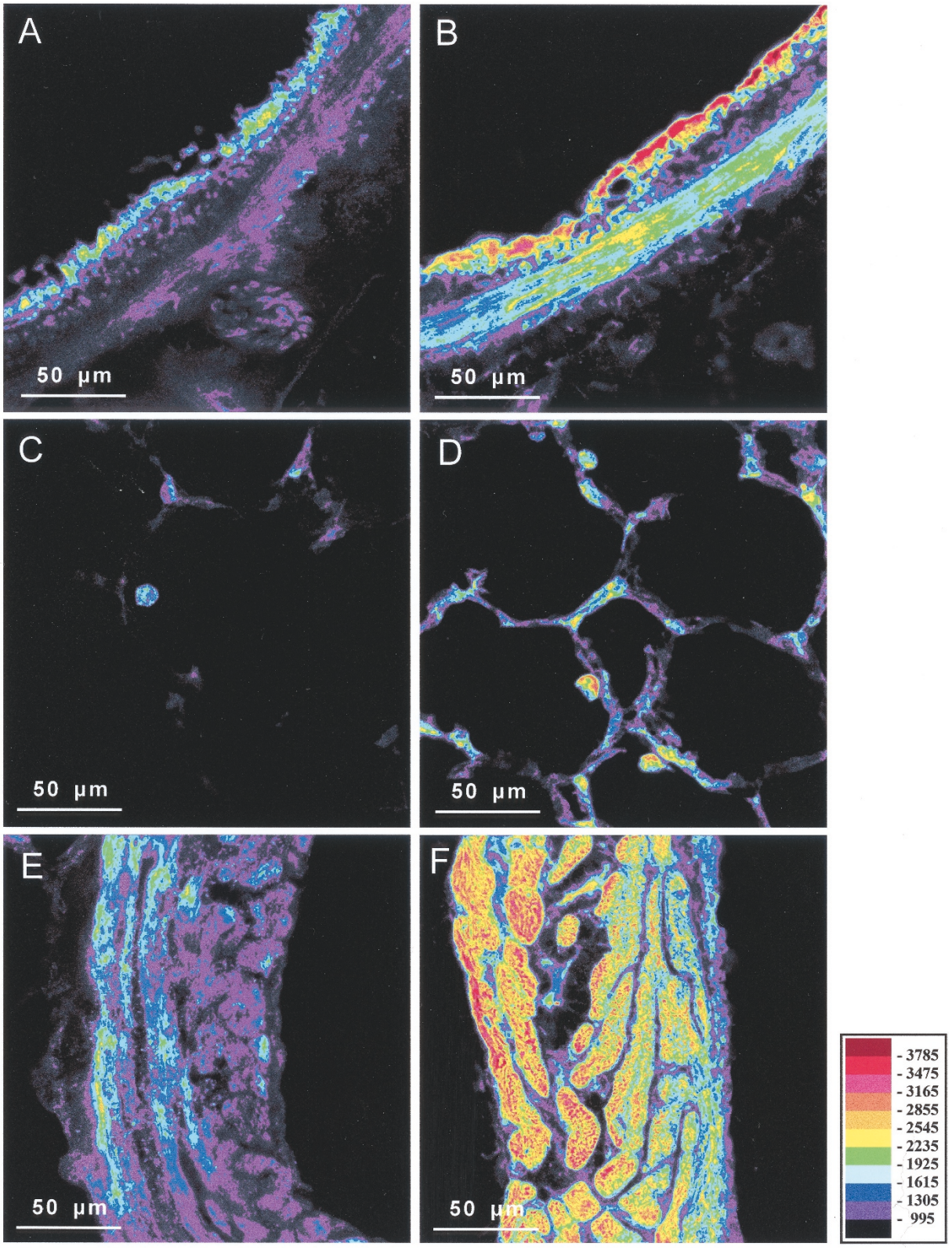

Figure 3.

Image analysis with pseudocolor depiction of immunohistochemical iNOS staining in control (A, C, and E) and LPS-stimulated rat lung tissue (B, D, and F). iNOS staining intensity was increased in bronchial epithelial cells and bronchial smooth muscle cells in response to LPS (B, 1000 ng/ml LPS, 1 hour). Within the lung parenchyma, alveolar macrophages and cells in the alveolar septum showed marked up-regulation of iNOS within 1 hour after LPS application (D, 10000 ng/ml LPS, 1 hour). Cardiac myocytes of large hilar veins display extensively increased iNOS expression in LPS-challenged lungs (F, 1000 ng/ml LPS, 2 hours).

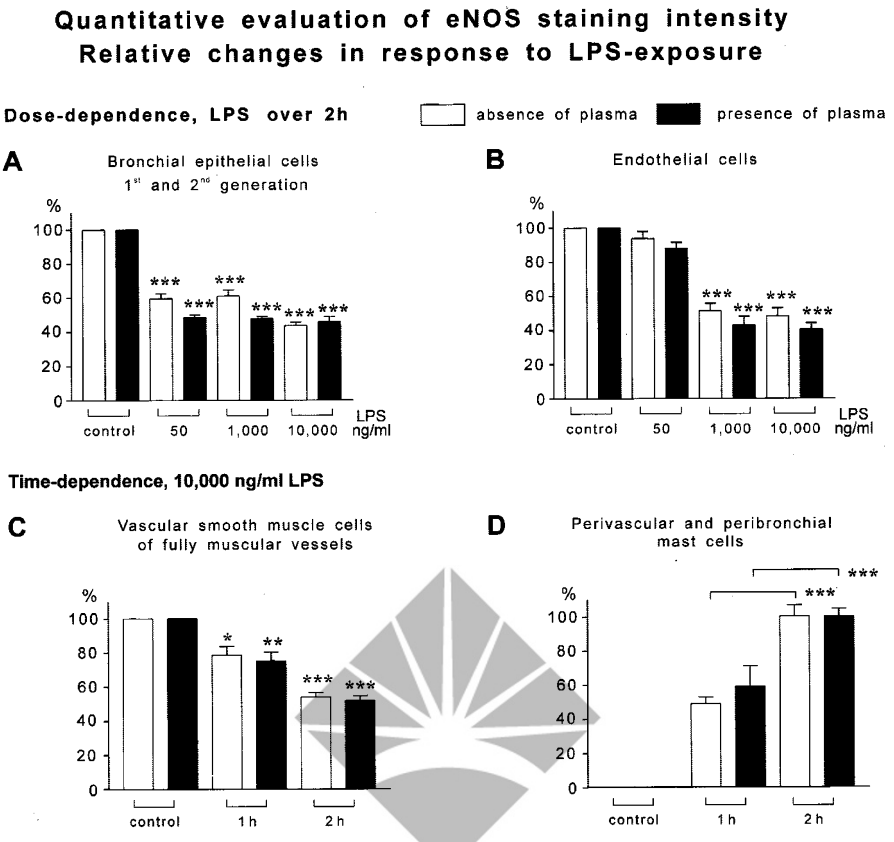

Figure 4.

Quantitative evaluation of immunohistochemical eNOS staining in response to LPS. Staining intensity is depicted in percent of gray scale values measured, with control lungs being set at 100% (except for D, where no control cell staining was noted). LPS challenge was performed in the absence (*open bars*) and in the presence (*closed bars*) of 1.5% plasma in the buffer perfusate. Time- and dose-dependent down-regulation (A to C) was noted in most cell types. In contrast increased expression of eNOS was found in mast cells (D). Mean ± SEM of five independent experiments each are given. $*p < 0.05$, $**p < 0.01$, $***p < 0.001$, as compared with control lung cells.

muscular vessels, iNOS expression was also increased (Table 2, a and b). In endothelial cells, newly induced iNOS was detected in groups receiving 50 ng/ml LPS both in groups perfused with buffer alone or buffer/plasma. Staining of endothelial cells was further increased in all groups receiving 1,000 or 10,000 ng/ml LPS. Perivascular leukocytes, which did not display positive iNOS staining in control groups or groups receiving low-dose LPS showed time-dependent up-regulation of iNOS in response to 1,000 and 10,000 ng/ml LPS (Table 2, a and b). There was no significant difference noted between buffer (Table 2a) and buffer/plasma (Table 2b) perfused lungs.

bNOS

Control Lungs and LPS-Challenged Lungs. In buffer- or buffer/plasma-perfused control lungs, strong bNOS immunostaining (Table 3, a and b) was detected in the bronchial epithelial cells of all bronchi, with strongest expression found in the smaller bronchi (Fig. 1A). In addition bNOS was present in perivascularly and peribronchially located mast cells. Next to alveolar macrophages, cells within the BALT exhibited positive immunostaining for bNOS. In addition in endothelial cells and VSMC of fully muscular vessels and myocytes of large veins at the lung hilum, a moderate expression of bNOS was detected. Nerve fibers exhibited intense bNOS immunoreactivity.

LPS treatment for either 1 or 2 hours, under both buffer- and buffer/plasma-perfusion conditions, did not change the pattern and intensity of bNOS immunostaining as compared with the control groups; data of selected experimental groups (1,000 ng/ml LPS, 2 hours; 10,000 ng/ml LPS, 1 hour and 2 hours) are presented in Table 3, a and b.

Discussion

The present study shows differential expression of all three types of isoenzymes in normal rat lung tissue. This was anticipated for the constitutive isoforms bNOS and eNOS (Asano et al, 1994; Kobzik et al, 1993; Shaul et al, 1994; Steudel et al, 1999), although an entire profile of cellular localization of both isoforms in lung tissue has so far not been shown. A recent study (Steudel et al, 1999) reported eNOS expression in epithelial cells, endothelial cells, and VSMC in normal rat lung tissue, which corresponds well with the data presented in this study. Alveolar macrophages and bronchial smooth muscle cells were, however, found to be negative for eNOS under base-

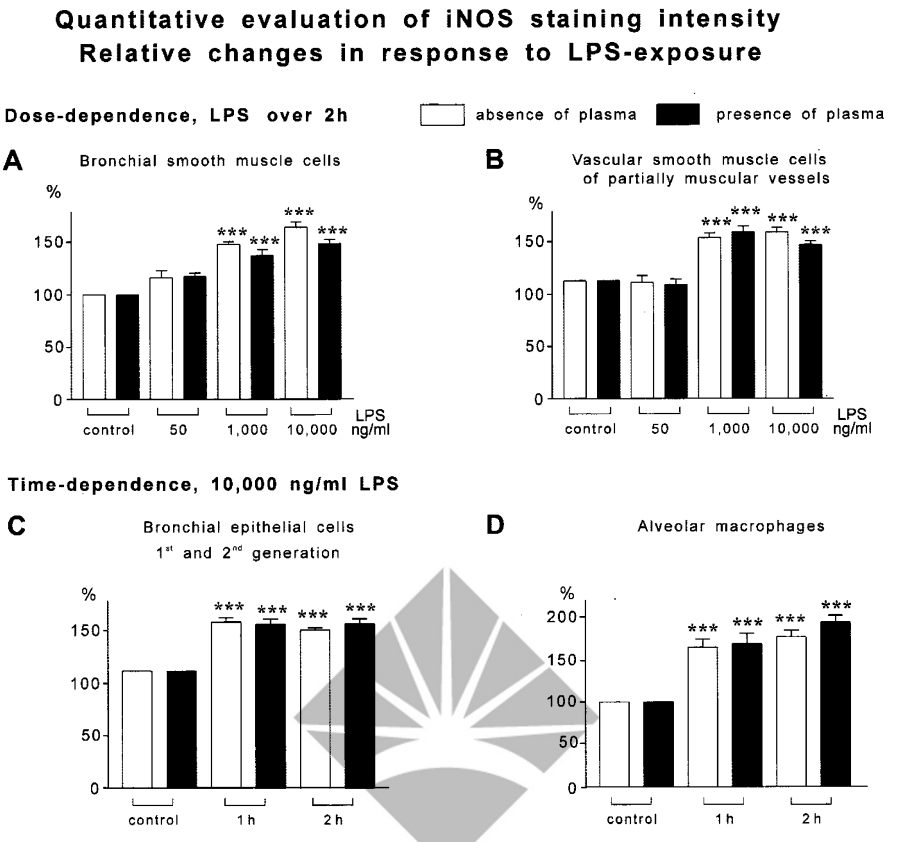

Figure 5.

Quantitative evaluation of immunohistochemical iNOS staining in response to LPS. Staining intensity is depicted in percent of gray scale values with control lungs being set at 100%. LPS challenge was performed in the absence (*open bars*) and in the presence (*closed bars*) of 1.5% plasma in the buffer perfusate. Time- and dose-dependent up-regulation (A to C) was noted in most cell types. Mean ± SEM of five independent experiments each are given. $*p < 0.05$, $**p < 0.01$, $***p < 0.001$, as compared with control lung cells.

line conditions in that study in contrast to the present investigation, which may be a result of different tissue treatment and embedding techniques (Steudel et al, 1999). Bronchial epithelial cells, endothelial cells, and VSMC of fully muscular vessels showed the highest staining intensity for eNOS under baseline conditions, as quantified by the currently used in situ microdensitometric method (Ermert et al, 2001). bNOS expression has been previously localized to nerve, epithelial, and endothelial cells in rat and human lung tissue (Asano et al, 1994; Kobzik et al, 1993). In addition we report here bNOS expression for alveolar macrophages and VSMC of fully muscular vessels, as well as myocytes of hilar veins. Perivascular and peribronchial macrophage-like cells, which in previous studies were shown to represent mast cells to some major extent (Ermert et al, 1998, 2000b), were shown to express bNOS but not eNOS or iNOS in nonstimulated rat lung tissue.

Similar to eNOS and bNOS, iNOS was found to be constitutively expressed in several lung cell types under baseline conditions in the present study. In accordance with previous observations (Asano et al, 1994; Steudel et al, 1999; Tracey et al, 1994; Watkins et al, 1997), iNOS expression was noted in bronchial epithelial cells of large and small airways. Such prominent constitutive iNOS expression in the bronchial epithelium may reflect the fact that this epithelium represents a barrier with a large external surface, being naturally exposed to airborne noxious and microbial agents even in the absence of lung infection. In addition, iNOS was expressed in bronchial smooth muscle cells, myocytes of pulmonary hilar veins (this study; Steudel et al, 1999), alveolar macrophages, cells within the BALT, and VSMC of partially and fully muscular vessels (this study). Microdensitometry of immunohistochemical staining intensity showed the most intensive iNOS expression in control lungs to be present in bronchial epithelial cells of large bronchi and in myocytes of large hilar veins. Endothelial cells were found to express eNOS and bNOS but not iNOS under baseline conditions. Differential expression of NOS isoenzymes was also found in myocytes of large hilar veins, which expressed iNOS and bNOS but not eNOS in control lungs. A complex cellular pattern of NO generation via different isoenzymes thus seems to contribute to NO-dependent physiologic regulations, which were suggested to include those of vascular tone, bronchial tone, neurotransmission, or immune defense (Gaston et al, 1994; Moncada et al, 1991).

Excess NO production, causing inappropriate vasodilation and peroxynitrite-related cellular injury, has been implicated in the pathogenesis of ARDS and septic lung failure (Beckman and Koppenol, 1996; van

der Vliet et al, 1999). Such NO overproduction was particularly attributed to the induction of iNOS in the lung tissue (Fujii et al, 1998; Warner et al, 1995; Wizemann et al, 1994). The current study does, however, demonstrate that the scenario is much more complex, with evidence being forwarded for a distinct regulation of both iNOS and eNOS in various lung cell types in response to endotoxin. eNOS expression was found to be down-regulated in all lung compartments, in nearly all cell types expressing this isoenzyme under baseline conditions. This was a striking finding of the present investigation, with underlying mechanisms for this type of regulatory response to endotoxin being currently unknown. In previous studies in cultured cells, a down-regulation of eNOS, triggered by increased NO production via LPS-induced iNOS expression, has been reported (Buga et al, 1993; MacNaul and Hutchinson, 1993; Schwartz et al, 1997). To our knowledge, such negative feedback regulation of eNOS expression by enhanced iNOS-derived NO formation has so far not been demonstrated in whole lung tissue but may well be operative to explain the disparate regulations of iNOS and eNOS in the present study. However, the down-regulation of eNOS in the vast majority of cell types in LPS-stimulated lungs may, of course, also be fully independent of enhanced iNOS-derived NO synthesis but may represent a direct downstream signaling event in endotoxin-exposed pulmonary cells. The underlying mechanism thus obviously deserves further elucidation.

Interestingly, de novo expression of eNOS was noted in mast cells in response to LPS. These cells were shown to express bNOS but not eNOS or iNOS in control lung tissue. The present observation is basically in line with earlier findings of TNF-mediated enhanced production of NO in cultured peritoneal and intestinal mast cells (Bissonnette et al, 1991), however, NO production was at that time not attributable to a certain NOS isoform. There is inconsistent information about NOS isoenzyme expression in mast cells of different organs: positive bNOS immunoreactivity has been reported for human skin mast cells (Shimizu et al, 1997), whereas both mouse myometrial (Huang et al, 1995) and connective tissue mast cells (Bidri et al, 1997) showed iNOS expression after hormonal or antigen stimulation. Further studies should address the issue of whether the up-regulation of eNOS in response to LPS in mast cells as opposed to other cell types is a lung-specific finding or is representative for mast cells of other organ origin.

In contrast to iNOS and eNOS, the expression of bNOS was found not to be altered in any of the different cell types in response to LPS stimulation. bNOS expression thus seems to be regulated in an entirely independent fashion, not comparable to that of eNOS and iNOS. Moreover, it does not seem to be affected by an increase in endogenous NO production, as expected because of the marked iNOS up-regulation, which is in line with previous in vitro studies (Buga et al, 1993; MacNaul and Hutchinson, 1993; Schwartz et al, 1997).

LPS exposure evoked increased expression of iNOS in particular in bronchial epithelial cells, bronchial smooth muscle cells, cells of the BALT, and alveolar macrophages. In the vascular system, iNOS was up-regulated in VSMC of fully muscular and partially muscular vessels and in myocytes of hilar veins. De novo expression in response to LPS, in a time- and dose-dependent fashion, was noted in endothelial cells and perivascularly located leukocytes. Increased expression of iNOS in leukocytes may well correspond to enhanced proinflammatory and cytotoxic activity of leukocytes during LPS-induced lung inflammation (Fujii et al, 1998; Liu et al, 1997). iNOS expression in pulmonary macrophages has been implicated in the regulation of the innate immunity system, which is indeed expected to respond to endotoxin challenge (Fujii et al, 1998; Liu et al, 1997). In cultured epithelial cells, increased production of NO has been observed to occur 8 to 24 hours after mitogen challenge and was associated with elevated iNOS mRNA and protein (Asano et al, 1994; Robbins et al, 1994; Watkins et al, 1997). In intact lungs, in contrast, increased concentrations of exhaled NO were reported as early as 2 to 3 hours after LPS treatment and were suggested to be an early marker of lung inflammation (Stewart et al, 1995). This study demonstrates significant increase in iNOS protein expression in bronchial epithelial cells within 1 to 2 hours after intravascular LPS application, which supports the notion that iNOS in particular contributes to excessive inflammatory NO generation in epithelial cells, and this is a very rapid response. Increase of iNOS in bronchial epithelium and alveolar macrophages has been correlated with enhanced nitrotyrosine detection, a marker for the formation of the powerful oxidant peroxynitrite, which is presumed to be largely responsible for many of the adverse effects of excessive NO generation (Beckman and Koppenol, 1996; Kristof et al, 1998; van der Vliet et al, 1999; Wizemann et al, 1994).

In addition to a marked increase of iNOS immunostaining intensity in the airways, we observed de novo expression of iNOS in endothelial cells and strong LPS-induced up-regulation of iNOS in VSMC within 1 to 2 hours after LPS application. Such iNOS response in the vascular system appeared thus again much earlier than was shown in cell culture studies, which reported induction of iNOS mRNA within 8 to 24 hours in LPS-treated VSMC (Johnson et al, 1994; MacNaul and Hutchinson, 1993; Nakayama et al, 1992), accompanied by significant peroxynitrite production in this cell type (Kristof et al, 1998). Excessive production of NO in the pulmonary vasculature via iNOS is thought to be a key mechanism in the pronounced systemic vasodilation of sepsis (Gaston et al, 1994, Moncada et al, 1991; Ullrich et al, 1999) and has also been implicated in sepsis-associated pulmonary edema via cytotoxic peroxynitrite formation (Hinder et al, 1999; Kristof et al, 1998). Studies in iNOS-deficient mice showed that these mice were protected from LPS-induced impairment of hypoxic pulmonary vasoconstriction and arterial oxygenation (Ullrich et al, 1999;

Weimann et al, 1999) and acute lung injury (Kristof et al, 1998). Thus, inappropriate NO formation from iNOS apparently causes loss of ventilation-perfusion matching including shunt flow in the lung vasculature, and the presently described up-regulation of iNOS in both endothelial and smooth muscle cells well explains such an event in septic lungs.

Summarizing the main immunohistochemical findings, the study shows a constitutive expression of all three NOS isoenzymes in lung tissue with a differential cellular pattern. Differences of NOS isoenzyme expression were particularly noted in endothelial cells, with a baseline expression of eNOS and bNOS and an additional induction of iNOS in response to LPS stimulation. Hilar vein cardiac muscle cells displayed positive staining for bNOS and iNOS, whereas smooth muscle cells of intrapulmonary vessels were positive for all three of the isoenzymes. A different expression pattern was noted in bronchial smooth muscle cells that expressed iNOS and eNOS but not bNOS. Under physiologic conditions bNOS was the only NOS type detected in mast cells; however, in response to LPS, eNOS was found to be de novo expressed. In perivascularly localized leukocytes, iNOS was induced and up-regulated after LPS stimulation. The differential cellular expression and regulation pattern observed may be a result of different cell-specific NOS isoenzyme-dependent cell functions involved in either physiologic or pathophysiologic mechanisms.

In contrast to a previous study on cellular Cox-2 expression in LPS-treated rat lungs (Ermert et al, 2000b), no difference in the cell type–specific expression of eNOS, bNOS, or iNOS between buffer- and buffer/plasma-perfused rat lungs was observed. This is a surprising finding, because CD14-negative cell types, such as bronchial smooth muscle cells, endothelial cells, epithelial cells of small bronchi, and large artery VSMC, showed LPS-induced Cox-2 up-regulation only in the presence of plasma constituents, with LBP and sCD14 assumed to be particularly important (Ermert et al, 2000b). LPS-induced NOS regulation may thus be suggested to engage different signal transduction pathways as compared with Cox-2 regulation in many cell types. Such a difference may include direct gene-regulatory response to endotoxin versus indirect response via LPS-induced cytokine synthesis, eg, TNF-α and IL-1 (Lamas et al, 1991; Nakayama et al, 1992; Robbins et al, 1994), which may then secondarily affect regulation of target systems independent of plasma constituents.

In conclusion, the present study demonstrates that LPS challenge of intact lungs exerts marked impact on the NOS regulation in many cell types. On the one hand, strong up-regulation of iNOS is noted in various cells of the vascular and bronchial system, which may provoke inflammatory events via peroxynitrite formation and which may affect the regulation of vascular tone, resulting in loss of ventilation-perfusion matching. On the other hand, eNOS is down-regulated in many cell types, suggesting hindrance of physiologic regulatory events with involvement of eNOS-based NO synthesis. Moreover, differential regulatory profiles as exemplified by eNOS and iNOS expression are noted in many immune-type cells. In contrast, no alteration of bNOS expression was noted in the LPS-treated lungs. Overall, the fundamental changes in cell-specific NOS regulation in response to endotoxin may well contribute to abnormalities in physiologic function in septic lung failure.

Materials and Methods

Reagents

Polyclonal antibodies against bNOS (SA-202), iNOS (SA-200), and eNOS (SA-201) were obtained from Biomol (Hamburg, Germany). Additional antibodies against iNOS and eNOS were purchased from Santa Cruz Biotechnology, Inc. (sc-651, sc-654, both polyclonal antibodies; Heidelberg, Germany) and BD Transduction Laboratories (catalog no. N30020, catalog no. N32020, both monoclonal antibodies; Franklin Lakes, New Jersey). The secondary antibodies goat anti-rabbit $F(ab)_2$ alkaline phosphatase (AP) conjugate and rabbit anti-goat $F(ab)_2$AP conjugate were obtained from Biotrend (Cologne, Germany). The Vector Red Substrate Kit was acquired from Vector Laboratories (Burlingame, California). All other biochemicals were obtained from Merck (Darmstadt, Germany).

Western blots confirming the specificity of the antibodies used in this study were performed with commercially obtained cell lysates and recombinant enzymes recommended for the detection of the specific NOS isoenzymes. For the detection of bNOS, an immunoblotting standard consisting of recombinant brain NOS protein from rat (catalog no. SW-109; Biomol GmbH, Hamburg, Germany) was used. The specificity for eNOS was tested on a recombinant eNOS enzyme isolated from a baculovirus overexpression system in SF9 cells (catalog no. 60880; Cayman Chemical, Ann Arbor, Michigan). For iNOS Western blotting, a cell lysate from RAW264.7 cells (mouse Abelson leukemia virus-transformed macrophages) stimulated with IFN-γ was used (catalog no. sc-2259; Santa Cruz Biotechnology).

Blotting of all three NOS isoforms was additionally performed with a commercial rat brain extract (catalog no. sc-2392; Santa Cruz Biotechnology) and homogenized rat lung tissue. Using the rat brain extract, all three isoforms could be strongly detected with specific bands, as stated in the literature. In the lung tissue homogenate, we detected specific bands with strong expression for eNOS and iNOS, and weak expression for bNOS, probably because the amount of bNOS was lower in the homogenate compared with the other NOS isoenzymes.

Animals

CD rats (Sprague Dawley) were obtained from Charles River (Sulzfeld, Germany). All experimental procedures were performed in conformity with the guidelines of the National Institutes of Health (Guide for the Care and Use of Laboratory Animals, NIH publication

no. 86–23, Revised 1985, United States Government Printing Office, Washington DC).

Lung Isolation and Perfusion

The rats (male, body weight 350 to 400 g) were deeply anesthetized with sodium pentobarbital (100 mg/kg body weight ip). After local anesthesia with 2% Xylocaine and a median incision, the trachea was dissected, and a tracheal cannula was immediately inserted. Subsequently, mechanical ventilation was started with 4% CO, 17% O, and 79% N (tidal volume 4 ml, frequency 65/minute, end expiratory pressure 3 cm H_2O) using a small animal respirator KTR-4 (Hugo Sachs Elektronik, March, Germany). A median laparotomy was performed, and subsequently the rats were anticoagulated with 1000 U of heparin. After midsternal thoracotomy the right ventricle was incised, a cannula was fixed in the pulmonary artery, and the apex of the heart was cut off to allow pulmonary venous outflow. Simultaneously, pulsatile perfusion with buffer solution was started. The buffer contained 2.4 mM $CaCl_2$, 1.3 mM $MgCl_2$, 4.3 mM KCl, 1.1 mM KH_2PO_4, 125.0 mM NaCl, and 25 mM $NaHCO_3$ as well as 13.32 mM glucose (pH ranged between 7.35 and 7.40).

The lungs were carefully excised, avoiding any damage, while being perfused with buffer solution, and suspended in an upright position. Next, a cannula was inserted through the left ventricle and fixed in the left atrium to obtain a closed perfusion circuit. Subsequently, lungs were placed in a temperature-equilibrated housing chamber (37° C) freely suspended from a force transducer.

After extensive rinsing of the vascular bed, the lungs were perfused in a recirculating manner with a pulsatile flow of 13 ml/minute. The alternate use of two separate perfusion circuits, each containing 100 ml, allowed the repetitive exchange of perfusion fluid. Perfusion pressure, ventilation pressure, and weight of the isolated organ were registered continuously. The left atrial pressure was set at 2 mm Hg under baseline conditions (0 referenced at the hilum) to guarantee zone III conditions at end expiration throughout the lung.

Lungs selected for the study were those that (a) had a homogeneous white appearance without signs of hemostasis or edema formation, (b) had pulmonary artery and ventilation pressures in the normal range, and (c) were isogravimetric during a steady-state period of 30 minutes.

Experimental Protocol

Rat lungs were perfused for about 5 minutes for washout of blood ($n = 5$). A total of 60 experiments with isolated rat lung perfusion were performed. In control experiments, rat lungs were perfused for 2 hours solely with buffer fluid ($n = 5$) or with buffer/plasma (1.5% rat plasma admixed). In additional experiments, LPS was admixed in concentrations of 50 mg/ml, 1,000 ng/ml, or 10,000 ng/ml to the recirculating buffer fluid. Subsequently, both 1-hour and 2-hour perfusion periods were performed. Challenge with LPS was performed in the absence or presence of 1.5% plasma (each group $n = 5$).

After termination of perfusion, the rat lungs were instilled with TissueTek OCT compound and frozen in liquid N_2. The rat lungs were dissected into tissue blocks from all lobes and stored at −80° C. Sections 10 μm in thickness were cut from frozen tissue blocks of both left and right lungs.

Immunohistochemistry

The sections were fixed for 5 minutes with 3% paraformaldehyde solution and washed in PBS (0.01 M, 150 mM NaCl, pH 7.6) for 3×5 minutes. They were treated for 15 minutes with a 1% Triton solution. The sections were preincubated in PBS containing 5% goat serum, 1% BSA, and 0.05% Tween-20 to block nonspecific binding. Overnight incubation with the polyclonal primary antibody in PBS containing 1% BSA, 0.05% Tween-20, was performed at 4° C (dilutions: bNOS [Biomol] 1:1000; iNOS [Biomol] 1:3000; iNOS [Santa Cruz] 1:100; eNOS [Biomol] 1:500; eNOS [Santa Cruz] 1:100]. The sections were then washed in PBS and incubated with goat anti-rabbit $F(ab)_2$AP conjugate diluted 1:2000 in the same dilution buffer overnight at 4° C. Afterward, washing of the sections in PBS for 3×5 minutes was performed. Subsequently, the sections were developed with a Vector Red Substrate Kit. Levamisole (2.5 mM) was added to inhibit endogenous AP activity. Counterstaining of the sections was performed with hematoxylin. Control staining was performed by omission of the primary antibody and substitution with nonspecific serum at the same dilution.

Image Analysis

The method has been previously described (Ermert et al, 2000a, 2000b, 2001). Briefly, an image analysis system consisting of a 12-bit cooled CCD camera (Sensys KAF 1400; Photometrics, Tucson, Arizona) mounted on a fully automated Leica DM RXA (Leica, Wetzlar, Germany) was used to digitize gray scale images to a Dual-Pentium 200 MHz host computer. Microscope settings were kept constant throughout all measurements (Objective: 40× oil, Leica PL Fluotar 40×/0.75). A stabilized 12V tungsten-halogen lamp (100 W) was used for illumination. Microdensitometry was performed with a custom-designed filter for absorbance measurement of the substrate Vector Red (central wave length 525 nm, half-band width 10 nm ± 2 nm) manufactured by Omega Optical, Inc. (Brattleboro, Vermont). Adjustment of all microscope settings was stored and recalled before measurement. Calibration of the measurement system with a reference slide was done before measurement. Gray scale images were digitized to 12-bit accuracy, resulting in an intensity scale ranging from 0 to 4095. Image analysis was performed by means of the image analysis program ImagePro 3.0 (Mediacybernetics, Silver Spring,

Maryland). For direct visualization of staining intensity, a pseudocolor scale with 11 colors was chosen, each representing an equal sector of the intensity scale, and applied to the images. Background measurement was performed to evaluate the influence of nonspecific staining and/or absorption of unstained tissue.

Five complete cross-sections per group from both right or left lung were measured. From each section, five images per stained structure (Table 1–3) were digitized, and the area of interest was manually defined. The mean gray values were automatically measured and subsequently transferred into the spreadsheet program EXCEL (Microsoft Corporation, Redmond, Washington).

Anatomic segments of the vascular tree were defined according to the classification described by Hislop and Reid (1978). In brief, elastic arteries and muscular and partially muscular vessels were distinguished by the structure of the vessel wall. Large arteries at the lung hilum were defined by the thickness of their muscle layer and the occurrence of elastic fibers, whereas hilar veins were identified by the cardiac muscle cells, which accompany the pulmonary veins of rats into the lung parenchyma (Hislop and Reid, 1978). A vessel was termed muscular or partially muscular when smooth muscle cells were observed in the subendothelial layer forming a muscular layer that surrounded the vessel either fully or partly, respectively. The vessels located in the preacinar regions were predominantly of a fully muscular type (associated with bronchioli and terminal bronchioli), whereas within the acinar region (associated with respiratory bronchioli and alveolar ducts) mainly partially muscular and nonmuscular vessels were found in accordance with previous data (Hislop and Reid, 1978).

Statistical Analysis

ANOVA was used to evaluate differences among different groups. A value of $p<0.05$ was considered significant. Data are given as mean ± SEM.

Acknowledgements

The authors thank Mrs. G. Müller (technical assistant) for excellent technical assistance. The authors are grateful to Dr. R. L. Snipes, Department of Anatomy, Giessen, for linguistically reviewing the manuscript.

References

Asano K, Chee CBE, Gaston B, Lilly CM, Gerard C, Drazen JM, and Stamler JS (1994). Constitutive and inducible nitric oxide synthase gene expression, regulation and activity in human lung epithelial cells. Proc Natl Acad Sci USA 91: 10089–10093.

Beckman JS and Koppenol WH (1996). Nitric oxide, superoxide and peroxynitrite: The good, the bad, and the ugly. Am J Physiol 271:C1424–C1437.

Bidri M, Ktorza S, Vouldoukis I, LeGoff L, Debre P, Guillosson JJ, and Arock M (1997). Nitric oxide pathway is induced by Fc epsilon RI and up-regulated by stem cell factor in mouse mast cells. Eur J Immunol 27:2907–2913.

Bissonnette EY, Hogaboam CM, Wallace JL, and Befus AD (1991). Potentiation of tumor necrosis factor-α-mediated cytotoxicity of mast cells by their production of nitric oxide. J Immunol 147:3060–3065.

Buga GM, Griscavage JM, Rogers NE, and Ignarro LJ (1993). Negative feedback regulation of endothelial cell function by nitric oxide. Circ Res 73:808–812.

El Samalouti VT, Schletter J, Chyla I, Lentschat A, Mamat U, Brade L, Flat HD, Ulmer AJ, and Hamann L (1999). Identification of the 80-kDa LPS-binding protein (LMP80) as decay-accelerating factor (DAF, CD55). FEMS Immunol Med Microbiol 23:259–269.

Ermert L, Ermert M, Goppelt-Struebe M, Walmrath D, Grimminger F, Steudel W, Ghofrani HA, Homberger C, Duncker H-R, and Seeger W (1998). Cyclooxygenase isoenzyme localization and mRNA expression in rat lungs. Am J Respir Cell Mol Biol 18:479–488.

Ermert L, Ermert M, Duncker H-R, Grimminger F, and Seeger W (2000a). In-situ localization and regulation of thromboxane A_2-synthase in normal and LPS-primed lungs. Am J Physiol 278:L744–L753.

Ermert L, Ermert M, Merkle M, Goppelt-Struebe M, Duncker H-R, Grimminger F, and Seeger W (2000b). Rat pulmonary cyclooxygenase-2 expression in response to endotoxin challenge: Differential regulation in the various types of cells in the lung. Am J Pathol 156:1275–1287.

Ermert L, Hocke ACH, Duncker H-R, Seeger W, and Ermert M (2001). Comparison of different detection methods in quantitative microdensitometry. Am J Pathol 158:407–417.

Frey EA, Miller DS, Jahr TG, Sundan A, and Bazil V (1992). Soluble CD14 participates in the response of cells to lipopolysaccharide. J Exp Med 176:1665–1671.

Fujii Y, Goldberg P, and Hussain SNA (1998). Contribution of macrophages to pulmonary nitric oxide production in septic shock. Am J Respir Crit Care Med 157:1645–1651.

Gaston B, Drazen JM, Loscalzo J, and Stamler JS (1994). The biology of nitrogen oxides in the airways. Am J Respir Crit Care Med 149:538–551.

Hamid Q, Springall DR, Riveros-Moreno V, Chanez P, Howarth P, Redington A, Bousquet J, Godard P, Holgate S, and Polack JM (1993). Induction of nitric oxide synthase in asthma. Lancet 342:1510–1513.

Hinder F, Stubbe HD, van Aken H, Waurick R, Booke M, and Meyer J (1999). Role of nitric oxide in sepsis-associated pulmonary edema. Am J Respir Crit Care Med 159:252–257.

Hislop A and Reid L (1978). Normal structure and dimensions of the pulmonary arteries in the rat. J Anat 125:71–83.

Huang J, Roby KF, Pace JL, Russell SW, and Hunt JS (1995). Cellular localization and hormonal regulation of inducible nitric oxide synthase in cycling mouse uterus. J Leukoc Biol 57:27–35.

Johnson BA, Lowenstein CJ, Schwarz MA, Nakayama DK, Pitt BR, and Davies P (1994). Culture of pulmonary microvascular smooth muscle cells from intraacinar arteries of the rat: Characterization and inducible production of nitric oxide. Am J Respir Cell Mol Biol 10:604–612.

Kobzik L, Bredt DS, Lowenstein CJ, Drazen J, Gaston B, Sugarbaker D, and Stamler JS (1993). Nitric oxide synthase in human and rat lung: Immunocytochemical and histochemical localization. Am J Respir Cell Mol Biol 9:371–377.

Kooy NW, Royall JA, Ye YZ, Kelly DR, and Beckman JS (1995). Evidence for in vivo peroxynitrite production in human acute lung injury. Am J Respir Crit Care Med 151:1250–1254.

Kristof AS, Goldberg P, Laubach V, and Hussain SNA (1998). Role of inducible nitric oxide synthase in endotoxin-induced acute lung injury. Am J Respir Crit Care Med 158:1883–1889.

Lamas S, Michel T, Brenner BM, and Marsden PA (1991). Nitric oxide synthesis in endothelial cells: Evidence for a pathway inducible by TNF-α. Am J Physiol 261:C634–C641.

Liu H-W, Anand A, Bloch K, Christiani D, and Kradin R (1997). Expression of inducible nitric oxide synthase by macrophages in rat lung. Am J Respir Crit Care Med 156:223–228.

MacNaul KL and Hutchinson NI (1993). Differential expression of iNOS and cNOS mRNA in human vascular smooth muscle cells and endothelial cells under normal and inflammatory conditions. Biochem Biophys Res Commun 196:1330–1334.

Michael JR, Barton RG, Saffle JR, Mone M, Markewith BA, Hillier K, Elstad MR, Campbell EJ, Toyer BE, Whatley RE, Liou TG, Samuelson WM, Carveth HJ, Hinson DM, Morris SE, Davis BL, and Day RW (1998). Inhaled nitric oxide versus conventional therapy: Effect on oxygenation in ARDS. Am J Respir Crit Care Med 157:1372–1380.

Moncada S and Higgs A (1993). The L-arginine-nitric oxide pathway. N Engl J Med 329:2002–2012.

Moncada S, Palmer RMJ, and Higgs EA (1991). Nitric oxide: Physiology, pathophysiology, and pharmacology. Pharmacol Rev 43:109–142.

Nakayama DK, Geller DA, Lowenstein CJ, Davies P, Pitt BR, Simmons RL, and Billiar TR (1992). Cytokines and lipopolysaccharide induce nitric oxide synthase in cultured rat pulmonary artery smooth muscle. Am J Respir Cell Mol Biol 7:471–476.

Payen DM (1998). Is nitric oxide inhalation a "cosmetic" therapy in acute respiratory distress syndrome? Am J Respir Crit Care Med 157:1361–1362.

Pugin J, Schürer-Maly C-C, Leturcq D, Moriarty A, Ulevitch RJ, and Tobias PS (1993). Lipopolysaccharide activation of human endothelial and epithelial cells is mediated by lipopolysaccharide-binding protein and soluble CD14. Proc Natl Acad Sci USA 90:2744–2748.

Qureshi ST, Lariviere L, Leveque G, Clermont S, Moore KJ, Gros P, and Malo D (1999). Endotoxin-tolerant mice have mutations in Toll-like receptor 4 (Tlr4). J Exp Med 189:615–625.

Robbins RA, Springall DR, Warren JB, Kwon OJ, Buttery LDK, Wison AJ, Adcock IM, Riveros-Moreno V, Moncada S, Polak J, and Barnes PJ (1994). Inducible nitric oxide synthase is increased in murine lung epithelial cells by cytokine stimulation. Biochem Biophys Res Commun 198:835–843.

Schwartz D, Mendonca M, Schwartz I, Xia Y, Satriano J, Wilson CB, and Blantz RC (1997). Inhibition of constitutive nitric oxide synthase (NOS) by nitric oxide generated by inducible NOS after lipopolysaccharide administration provokes renal dysfunction in rats. J Clin Invest 1400:439–448.

Shaul PW, North AJ, Wu LC, Wells LB, Brannon TS, Lau KS, Michel T, Margraf LR, and Star RA (1994). Endothelial nitric oxide synthase is expressed in cultured human bronchiolar epithelium. J Clin Invest 94:2231–2236.

Sherman TS, Chen Z, Yuhanna IS, Lau KS, Margraf LR, and Shaul PW (1999). Nitric oxide synthase isoform expression in the developing lung epithelium. Am J Physiol 276:L383–L390.

Shimizu Y, Sakai M, Umemura Y, and Ueda H (1997). Immunohistochemical localization of nitric oxide synthase in normal skin: Expression of endothelial-type and inducible-type nitric oxide synthase in keratinocytes. J Dermatol 24:80–87.

Steudel W, Watanabe M, Dikranian K, Jacobson M, and Jones RC (1999). Expression of nitric oxide synthase isoforms (NOS II and NOS III) in adult rat lung in hyperoxic pulmonary hypertension. Cell Tissue Res 295:317–329.

Stewart TE, Valenza F, Ribeiro SP, Wener AD, Volgyesi G, Brendan J, Mullen M, and Slutsky AS (1995). Increased nitric oxide in exhaled gas as an early marker of lung inflammation in a model of sepsis. Am J Respir Crit Care Med 151:713–718.

Tobias PS, Soldau K, and Ulevitch RJ (1989). Identification of a lipid A binding site in the acute phase reactant lipopolysaccharide binding protein. J Biol Chem 264:10867–10871.

Tracey WR, Xue C, Klinghofer V, Barlow J, Pollock JS, Förstermann U, and Johns RA (1994). Immunochemical detection of inducible NO synthase in human lung. Am J Physiol 266:L722–L727.

Troncy E, Collet J-P, Shapiro S, Guimond J-G, Lair LB, Ducruet T, Fancoer M, Charbonneau M, and Blaise G (1998). Inhaled nitric oxide in acute respiratory distress syndrome: A pilot randomized controlled study. Am J Respir Crit Care Med 157:1483–1488.

Ulevitch RJ (1993). Recognition of bacterial endotoxins by receptor-dependent mechanisms. Adv Immunol 53:267–289.

Ullrich R, Bloch KD, Ichinose F, Steudel W, and Zapol WM (1999). Hypoxic pulmonary blood flow redistribution and arterial oxygenation in endotoxin-challenged NOS2-deficient mice. J Clin Invest 104:1421–1429.

van der Vliet A, Eiserich JP, Shigenaga MK, and Cross CE (1999). Reactive nitrogen species and tyrosine nitration in the respiratory tract: Epiphenomena or a pathobiologic mechanism of disease? Am J Respir Crit Care Med 160:1–9.

Warner RL, Paine R III, Christensen PJ, Marletta MA, Richards MK, Wilcoxen SE, and Ward PA (1995). Lung sources and cytokine requirements for in vivo expression of inducible nitric oxide synthase. Am J Respir Cell Mol Biol 12:649–661.

Watkins DN, Peroni DJ, Basclain KA, Garlepp MJ, and Thompson PJ (1997). Expression and activity of nitric oxide synthases in human airway epithelium. Am J Respir Cell Mol Biol 16:629–639.

Weimann J, Bloch KD, Takata M, Steudel W, and Zapol WM (1999). Congenital NOS2 deficiency protects mice form LPS-induced hyporesponsiveness to inhaled nitric oxide. Anesthesiology 91:1744–1753.

Wizemann TM, Gardner CR, Laskin JD, Quinones S, Durham SK, Goller NL, Ohnishi ST, and Laskin DL (1994). Production of nitric oxide and peroxynitrite in the lung during acute endotoxemia. J Leukoc Biol 56:759–768.

Xue C, Reynolds PR, and Johns RA (1996). Developmental expression of NOS isoforms in fetal rat lung: Implications for transitional circulation and pulmonary angiogenesis. Am J Physiol 270:L88–L100.

Yang R-B, Mark MR, Gray A, Huang A, Xie MH, Zhang M, Goddard A, Wood WI, Gurney AL, and Godowski PJ (1998). Toll-like receptor-2 mediates lipopolysaccharide-induced cellular signalling. Nature 395:284–288.